Food Hydrocolloids 71 (2017) 158–167

Contents lists available at ScienceDirect

Food Hydrocolloids

journal homepage: www.elsevier.com/locate/foodhyd

Protein-polysaccharide associative phase separation applied to obtain a linoleic acid dried ingredient

Osvaldo E. Sponton [a, b], Adrián A. Perez [a, b], Liliana G. Santiago [b, *]

[a] Consejo Nacional de Investigaciones Científicas y Técnicas de la República Argentina (CONICET), Argentina
[b] Área de Biocoloides y Nanotecnología, Instituto de Tecnología de Alimentos, Facultad de Ingeniería Química, Universidad Nacional del Litoral, 1 de Mayo 3250 (3000), Santa Fe, Argentina

ARTICLE INFO

Article history:
Received 22 November 2016
Received in revised form
19 April 2017
Accepted 17 May 2017
Available online 18 May 2017

Keywords:
Ovalbumin nanoparticles
Gum arabic
High methoxyl pectin
Linoleic acid
Encapsulation
Powder

ABSTRACT

This paper gives experimental information about the application of protein-polysaccharide associative phase separation to produce a dried ingredient (powder) of linoleic acid (LA). Powder production process consisted in: (i) LA binding to a well-characterized ovalbumin nanosized heat-induced aggregate (OVAn) to form LA-OVAn complexes in solution, (ii) polysaccharides (PS) addition to promote the associative phase separation of LA-OVAn complexes, and (iii) freeze-drying of the precipitated phase in order to obtain LA-OVAn-PS powders. For this, OVAn and anionic PS (gum Arabic -GA- and high methoxyl pectin -HMP-) mixed systems were studied at different OVAn-PS concentration ratio ($R_{OVAn:PS}$) and aqueous medium pH by means of a complementary techniques set: optical density at 400 nm (as a measure of turbidity), zeta potential and biopolymer phase composition determination. Biopolymer associative phase separation process was described in terms of OVAn and PS separation yield (Y_{OVAn} and Y_{PS}, respectively) and PS content necessary to precipitate OVAn (PS_p). Y_{OVAn} and PS_p results suggest that $R_{OVAn:PS}$ 1:1 and 2:1 for OVAn-GA and OVAn-HMP systems, respectively, and pH 3.0 were the most suitable conditions to obtain LA-OVAn-PS freeze-dried powders. Powders water dispersibility and LA oxidative stability were evaluated over 13 days (expressed as non-deteriorated LA percent -LA_{ND}-). Results revealed that water dispersion behavior of LA-OVAn-HMP powder was better than LA-OVAn-GA; besides it has the highest LA_{ND} (~80%) at the 13 day. These experimental findings highlighted that OVAn-PS associative phase separation was a convenient strategy, besides this information could be relevant to produce a LA functional ingredient.

1. Introduction

Currently, the encapsulation of polyunsatured fatty acids (PUFAs) employing biopolymer nanoparticles constitutes an interesting topic in food science and technology field. Protein-polysaccharide electrostatic complexes have been proposed as encapsulating matrices due to their relatively easy production and their advantages on PUFAs molecular preservation (Santiago & Castro, 2016; Semenova, 2016). In these supramolecular structures, protein is the vehicle in which PUFA is attached forming an inclusion complex (Joye & McClements, 2014), whereas polysaccharide (PS) is electrostatically deposited onto the surface of the protein-PUFA nanocomplex, conferring to the ligand additional protection against injurious factors, e.g. oxygen, UV radiation, etc. (Perez, Sponton, Andermatten, Rubiolo, & Santiago, 2015; Zimet & Livney, 2009). Several proteins were assayed as PUFAs vehicles (and other lipophilic bioactive compounds), e.g. β-lactoglobulin (Perez, Andermatten, Rubiolo, & Santiago, 2014; Zimet & Livney, 2009), β-conglicinin (David, Zagury, & Livney, 2015), α-lactalbumin (Kehoe & Brodkorb, 2014), zein, gliadin (Joye, Davidov-Pardo, Ludescher, & McClements, 2015) and ovalbumin (OVA) and their nanosized heat-induced aggregates (OVAn) (Sponton, Perez, Carrara, & Santiago, 2015a,b). Recently, OVA and OVAn were evaluated as nanocarrier systems to vehiculize linoleic acid (LA), which was taken as a model PUFA. Data strongly highlighted the increased LA binding ability of OVAn due to a greater exposition of hydrophobic residues promoted by thermal denaturation (Sponton et al., 2015a,b). Furthermore, Sponton Perez, Carrara and Santiago (2016) pointed out the appropriate conditions to produce LA-OVAn nanocomplexes, considering stoichiometric, kinetic and thermodynamic aspects.

* Corresponding author.
E-mail address: lsanti@fiq.unl.edu.ar (L.G. Santiago).

http://dx.doi.org/10.1016/j.foodhyd.2017.05.020
0268-005X/

Nevertheless, in order to contribute to the knowledge about how is the vehiculization process of PUFAs, a study about OVAn-PS interactions in aqueous solution could be required. Hence, in this work, the interactions among OVAn with two PS commonly used in the food sector (gum arabic, GA, and high methoxyl pectin, HMP) is proposed.

Gum Arabic is an arabinogalactan-type polysaccharide exuded from the African tree *Acacia senegal*. It is composed by six carbohydrate moieties. The polysaccharides units are linked to a common polypeptide chain forming a "wattle blossom"-type structure. GA is negatively charged at pH > 2.2, whereas below this pH carboxyl group dissociation is suppressed (Weinbreck, de Vries, Schrooyen, & de Kruif, 2003).

Pectins are linear polysaccharides with negative charges due to galacturonic acid dissociation (Wicker, Kim, Kim, Thirkield, & Lin, 2014; de Jong & van de Velde, 2007). Pectins are divided in two groups according to the degree of methyl esterification (DE) of carboxylic groups. Pectins with DE > 50% are called high methoxyl pectins (HMP), whereas low methoxyl pectins (LMP) have DE < 50% (Ptaszek et al., 2015). The carboxylic groups along the backbone have a pKa ~3.6 (Humblet-Hua, Scheltens, van der Linden, & Sagis, 2011).

In terms of aqueous medium pH, different macromolecular interactions between protein and anionic PS could take place. In general, at pH > pI > pKa, mutual repulsion between protein and PS is due to the negative charges of both biopolymer. This behavior is known as cosolubility (Davidov-Pardo, Joye, & McClements, 2015; de Kruif, Weinbreck, & De Vries, 2004). When pH is around pI, association between protein cationic groups and PS anionic groups promotes electrostatic complexes formation. In general, the repulsion between PS residual negative charges promotes soluble complexes (Perez et al., 2015). These two kinds of interactions (cosolubility and soluble complexes) result in colloidal stable systems showing only one phase. However, at pKa < pH < pI, complex coacervation could occur due to the strong electrostatic attraction, and the complete neutralization of biopolymer charges (Weinbreck et al., 2003; Perez et al., 2014). This condition drives to associative phase separation, being one phase rich in both biopolymers and the other rich in solvent (Davidov-Pardo et al., 2015; Niu et al., 2014). Moreover, when pH is reduced too far, the coacervates precipitate, because they become closely packed together. Lastly, when pH < pKa cosolubility condition is newly reached due to the loss of charges of the polysaccharides (Davidov-Pardo et al., 2015). Associative phase separation involves both complex coacervation and precipitation. It is important to highlight that not only electrostatic interactions are involved in all these interactions. Hydrogen bonding, van der Waals and hydrophobic forces can also occur, depending on the biopolymer conformation and aqueous medium variables, e.g. pH and ionic strength (Fioramonti, Perez, Aringoli, Rubiolo, & Santiago, 2014; McClements, 2006).

On the other hand, in relation to biopolymer associative interactions, it is important to note that the strategy to produce biopolymer nanoparticles through protein-polysaccharide complexes is generally used at diluted biopolymer solution. Hence, it seem to be more appropriate, e.g., for PUFAs enriched beverages formulation (Zimet & Livney, 2009), limiting applications to others food matrices. The production and applications of nanoparticles in industry is still incipient, so an interesting alternative to increase their usage could be the production of biopolymer nanoparticles under powder form. However, this fact leads to the challenge of removing great water contents. In this sense, a strategy involving protein-polysaccharide associative phase separation could be adequate to concentrate biopolymer nanoparticles solutions, and consequently, to reduce energy consumption on the drying process. At the same time, PS addition could confer a protective effect on PUFAs-protein nanocomplexes (Zimet & Livney, 2009).

In this framework, the aim of this paper was to study the experimental conditions in which an associative phase separation process of OVAn-PS mixtures could take place in order to concentrate LA-OVAn nanocomplex solutions and to obtain a LA dried ingredient (powder). The associative phase separation process was evaluated in terms of: (i) two anionic PS, gum arabic (GA) and high methoxyl pectin (HMP), (ii) OVAn:PS concentration ratio ($R_{OVAn:PS}$) and (iii) aqueous medium pH. After this screening, the more appropriate conditions to promote associative phase separation were chosen and LA-OVAn-PS freeze-dried powders were obtained. In order to probe the success of the associative phase separation process, the dispersibility in water and oxidative stability of the freeze-dried powders were analyzed over 13 days. It is important to remark that there are not studies about protein-polysaccharide associative phase separation process applied to encapsulate PUFAs under powder form. Therefore, the present paper will give relevant information about technological aspects that could be useful to produce dried ingredients based on PUFAs.

2. Materials and methods

2.1. Materials

OVA (product A5503, purity 98% according to agarose gel electrophoresis) and LA samples were purchased from Sigma (USA). LA was kept under a N_2 atmosphere at −18 °C according to manufacturer advice. GA (*Acacia senegal*) was kindly supplied by Centro Enológico Rivadavia S.A. (Argentina). Its composition in dry basis (wt. %) was: 89.5% fiber, 4.5% sugar, 2.9% protein, 3.1% ash, and 0.05% fat. HMP (DE: 66–70%) was kindly supplied by Cargill™ (Argentina). Its composition in dry basis (wt. %) was: 74.7% fiber, 20.9% sugar, 2.2% protein, 2.2% ash and 0% fat. Deionized water (conductivity < 0.056 μS/cm) was used.

The solutions of Lowry Method to determine protein were (Hartree, 1972):

Solution A (1 g sodium-potassium tartrate, 50 g sodium carbonate and 250 mL 1 N NaOH diluted at 500 mL).
Solution B (2 g sodium-potassium tartrate, 1 g CuSO4·7H2O, 10 mL 1 N NaOH, and 90 mL water).
Solution C (1 volume of Foulin-Ciocalteu reagent diluted with 15 vol of water)

2.2. Ovalbumin nanoparticles production

OVAn was obtained by heat treatment (85 °C, 5 min) of 10 g/L OVA dispersion, at pH 7.5 and 50 mM NaCl, according to a previous work (Sponton et al., 2015a). It is important to remark that OVAn showed a monomodal particle size distribution (determined by dynamic light scattering, DLS) with a peak at 79 nm, and 0.208 polydispersity index (PdI), as it was reported in Sponton et al. (2015a).

2.3. Protein-polysaccharide interaction

In order to know the experimental conditions in which associative phase separation occur, a study of the macromolecular interactions in solution between OVAn and PS (GA and HMP) was firstly conducted. Results derived from this study were subsequently applied to concentrate LA-OVAn-PS particles solution. For this, OVAn dispersion (10 g/L) was diluted at 2 g/L with 50 mM pH 7.0 potassium phosphate buffer. Furthermore, GA and HMP stock solutions were prepared dispersing the proper PS amount in

deionized water at 0.6, 1.0 and 2.0 g/L concentration. These ones were used to prepared OVAn-PS systems at the following concentration ratios ($R_{OVAn:PS}$): 3.3:1, 2:1 and 1:1 (g/L). After mixing, pH systems were gradually decreased under magnetic stir from 7.0 up to 2.5, by decreasing 0.5 pH units with addition of HCl 1 M. When pH value was stabilized, aliquots were taken for further analysis (turbidity, zeta potential and phase composition determination), which are described below. An OVAn solution (without PS) was also assayed as control.

2.3.1. Turbidity measurements

Optical density (OD) at 400 nm (as a measure of turbidity) of OVAn-PS solutions were determined using a Jenway 7305 Spectrophotometer (UK) equipped with a 1 cm quartz cell (Fioramonti et al., 2014). In order to register initial turbidity measurements, tubes with samples were shaken and OD values were immediately determined. Measurements were performed at room temperature (around 20 °C) in duplicate.

2.3.2. Zeta potential

Zeta potential values for OVAn-PS systems were determined in a Zetasizer Nano ZS90 equipment (Malvern Instruments Ltd., UK). This instrument measures the electrophoretic mobility distribution by means of laser Doppler velocity technique. Zeta potential values were calculated according to the Smoluchowski model, using the software provided by the equipment. OVAn, GA and HMP pure systems were also assayed as controls. An estimation of the isoelectric point (pI) values was obtained from zeta potential *versus* pH curves, by fitting experimental data to a linear regression model. Determinations were performed at 25 °C in duplicate.

2.3.3. Biopolymer phase composition

In order to determine the biopolymer compositions of the phases after the associative phase separation, a centrifugation step at 5000 g for 15 min was performed. Subsequently, supernatant was carefully separated from the pellet. The OVAn and PS contents in supernatant were determined through Lowry's and phenol-sulfuric acid methods, respectively. These methods are commonly used in the determination of phase composition of protein/PS mixtures (Agbenorhevi & Kontogiorgos, 2010; Li et al., 2016; Spada, Marczak, Tessaro, & Cardozo, 2015). Then, OVAn and PS contents in the pellet were estimated as the difference among the total and supernatant contents.

OVAn content was determined by Lowry's method, adding 0.9 mL of solution A to 1 mL of diluted sample and then samples were heated at 50 °C during 10 min. Afterwards, 0.1 mL of solution B and 3 mL of solution C were added, and the mixture was again heated at 50 °C for 10 min. Finally, absorbance at 750 nm was registered (Hartree, 1972). Calibration curve for OVAn at 0–0.015 g/L concentration range was performed. Then, OVAn fraction in the pellet was calculated and defined as OVAn separation yield (Y_{OVAn}, %) (Eq. (1)):

$$Y_{OVAn}(\%) = \frac{OVAn\ in\ pellet(g)}{Total\ OVAn\ in\ system(g)} \cdot 100 \quad (1)$$

On the other hand, the determination of PS content was carried out by means of phenol-sulfuric acid method (Dubois, Gilles, Hamilton, Rebers, & Smith, 1956), by adding 25 μL of 80 % wt. phenol solution to 1 mL of diluted supernatant sample. Then, 2.5 mL of concentrated sulfuric acid solution was added. After cooling, absorbance at 480 nm was registered. Calibration curves for GA and HMP in the range of 0–0.12 g/L concentration were performed. PS fraction in the pellet was calculated and defined as PS separation yield (Y_{PS}, %) (Eq. (2)):

$$Y_{PS}(\%) = \frac{PS\ in\ pellet(g)}{PS\ in\ system(g)} \cdot 100 \quad (2)$$

Finally, PS amount related to OVAn in the pellet (PS_p, %), was calculated as (Eq. (3)):

$$PS_p = \frac{PS\ in\ pellet\ (g)}{OVAn\ in\ pellet\ (g)} \cdot 100 \quad (3)$$

2.4. Production and characterization of LA-OVAn-PS powders

According to results derived from the study described in section 2.3, the more appropriate conditions to promote associative phase separation of protein-polysaccharide mixtures were selected in order to obtain a pellet rich in LA-OVAn-PS. Procedure described by Sponton et al. (2016) was used to obtain LA-OVAn nanocomplexes. Briefly, an ethanolic LA solution was added to 50 mM potassium phosphate buffer, pH 7. After that, a volume of OVAn dispersion was added, to obtain LA:OVAn concentration ratio of 0.28:1 (g/L). The system was left to reach equilibrium during 30 min. Then, a volume of PS dispersion was added, and the aqueous medium pH was adjusted to 3.0. After that, a centrifugation step at 5000 g for 15 min was applied. Supernatant was separated and the pellet was freezed at −80 °C. Finally, a lyophilization process was performed in a Freeze Dryer Christ® Alpha 1–4 LD plus (UK). All freeze-dried powders were kept in a N_2 atmosphere at −18 °C until further analysis. A system without PS was also included as a control.

2.4.1. Powder dispersibility in water

LA-OVAn and LA-OVAn-PS freeze-dried powders were dispersed in water at 2 g/L concentration. After 24 h hydration, dispersion pH was measured, and then it was adjusted to 7.0 with 0.5 M NaOH in order to achieve cosolubility condition. Dispersions were equilibrated for 24 h in repose. Then, dispersions were centrifuged at 2000 g for 15 min, and particle size distribution (PSD) was determined by DLS (Zetasizer Nano ZS90, Malvern Instruments Ltd., UK). Refractive indexes used for aqueous solvent and protein aggregates were 1.33 and 1.50, respectively (Sponton et al., 2015a).

2.4.2. Determination of encapsulation parameters

In order to determine the encapsulation parameters: loading capacity (LC), encapsulation efficiency (EE) and encapsulation yield (EY) for freeze-dried powders, total LA (LA_T) and free LA (LA_{free}) contents were quantified by RP-HPLC, using a Perkin Elmer chromatographer (USA) equipped with a pump (Series 2000), a UV/Vis detector (785A) and an interface (NCI 900). Characteristics of C18 (ODS) Symmetry300™ column (Waters Corp., USA) were: 250 mm length, 4.6 mm inner diameter, 5 μm particle size, 30 nm pore size, was used. RP-HPLC experimental conditions were defined according to Li, Gu, Kelder, and Kopchick (2001) and Zimet and Livney (2009). LA detection was performed at 195 nm wavelength, and a linear gradient from 30% water +70% acetonitrile (phase A) to 100% acetonitrile (phase B) was applied over 15 min. Subsequently, 100% acetonitrile was maintained over 5 min. Acetic acid solution (0.12 vol %) was added to both mobile phases. Calibration curve for LA standard in methanol solution at 0–140 mg/L concentration range was done.

In order to quantify LA_T, powder samples were digested according to Gallardo et al. (2013). Briefly, 1 mL of HCl 8 M solution was added to 0.02 g sample in glass tubes and then they were placed in a water thermostatic bath (Dalvo instruments, BTMP model) at 70 °C. Then, bath temperature was set and kept at 100 °C

over 30 min. After cooling, 2.5 mL hexane were added to the tubes, and they were mixed for 1 min in vortex. A centrifugation step at 20 g for 15 min was performed and 0.5 mL hexane phase was evaporated under N_2 stream. Finally, methanol was added and the resultant solution was injected into the chromatographer. According to Joye and McClements (2014), LA_T was referred as loading capacity (LC).

For LA_{free} determination, 1 mL hexane was mixed with 0.02 g sample for 1 min on vortex mixer. Then, a centrifugation step at 10,000 g for 30 min was applied and 0.5 mL hexane phase was evaporated under N_2 stream. Methanol was added and resultant solution was injected into the chromatographer. LA_T and LA_{free} were expressed in terms of powder mass percent. Encapsulated LA amount (LA_E) was calculated as the difference between LA_T and LA_{free} (Eq. (4)):

$$LA_E = LA_T - LA_{free} \quad (4)$$

On the other hand, encapsulation efficiency (EE) and yield (EY, %) parameters were calculated according to Joye and McClements (2014) (Eqs. (5) and (6), respectively):

$$EE = LA_E/LA_T \quad (5)$$

$$EY(\%) = \frac{LA_E \cdot m}{LA_0} \quad (6)$$

where m is the total powder mass, and LA_0 is total LA content used to prepare freeze-dried powders (0.28 g).

2.4.3. LA oxidative stability assay

Oxidative **s**tability assay for LA-OVAn-PS and LA-OVAn freeze-dried powders was evaluated under ambient air exposition at 40 °C. This condition was selected in order to undergo the samples to an accelerated shelf-life stress condition (Zimet & Livney, 2009). For this, 0.02 g powder was placed in capped glass tubes, which were kept in darkness at 40 °C. Samples were taken at 1, 2, 5 and 13 days, and LA_T was determined according the procedure described in section 2.4.2. As a measure of LA oxidative stability, the non-deteriorated LA percent (LA_{ND}) was calculated according to Eq. (7):

$$LA_{ND}(\%) = \frac{LA_T^t}{LA_T^0} \quad (7)$$

Where LA_T^t is the total LA content at time t, while LA_T^0 is the initial total LA content in freeze-dried powders.

2.5. Statistical analysis

Significant differences were determined by ANOVA with a 95% significance level ($p < 0.05$). In order to elucidate significant differences between data groups, the least significant difference test (LSD) was performed, using R software with R-Studio interface.

3. Results and discussion

3.1. OVAn-PS interactions in solution

3.1.1. Turbidity and zeta potential analysis

Experimental conditions in which associative phase separation of OVAn-PS mixtures take place were firstly examined. Figs. 1 and 2 show the effect of aqueous medium pH on OD at 400 nm (as a measure of turbidity) and zeta potential of OVAn-PS systems, respectively. Moreover, Fig. 3 shows the visual appearances of the different systems at initial time and after 24 h. As visual

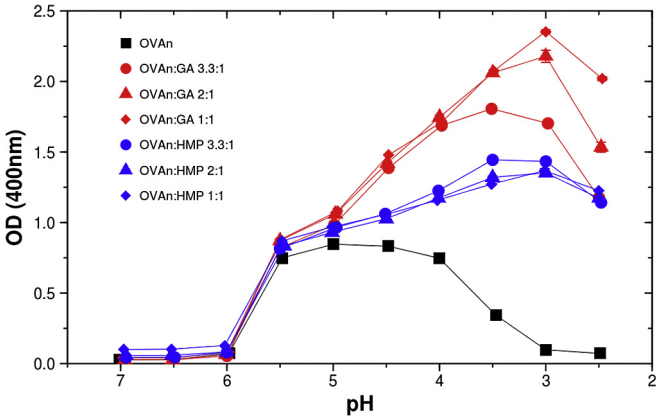

Fig. 1. Initial turbidity (OD at 400 nm) as a function of pH for OVAn, OVAn-GA and OVAn-HMP systems.

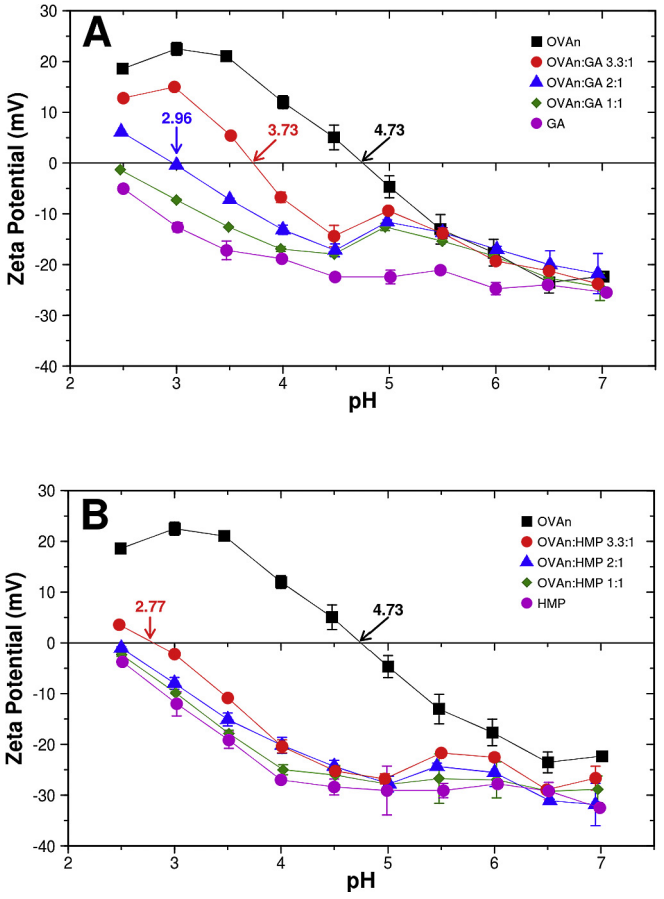

Fig. 2. Z-Potential *versus* pH profiles at different OVAn-PS relations. **A**:OVAn-GA; **B**:OVAn-HMP.

appearances were similar among the different $R_{OVAn:PS}$, only the 1:1 one is showed. It is important to remark that either OVAn or OVAn-PS systems with OD values higher than 0.25, showed macroscopic associative phase separation. This means that, in case of OVAn-PS systems, turbidity development would not be related to the formation of soluble complexes. On the contrary, Perez et al. (2015) reported the formation of soluble complexes between HMP and β-lactoglobulin, which formed a colloidal stable turbid system. In the present work, we hypothesize that OVAn-PS complexes

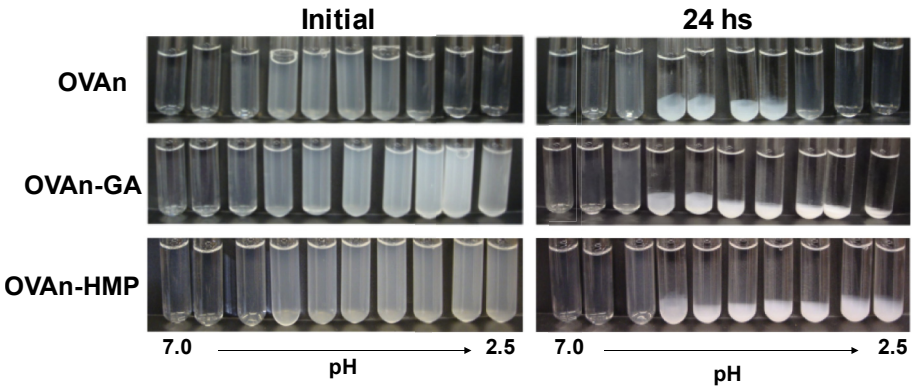

Fig. 3. Visual appearance of OVAn-PS systems at $R_{OVAn:PS}$ 1:1 (g/L). The pH decrease was made by 0.5 units.

aggregate, and when have enough size precipitate.

For OVAn system, OD was almost zero over a pH rage of 7.0–6.0 (Fig. 1). The maximum OD values were observed between pH 5.5 and 4.0, and then OD values gradually decreased (pH 4.0–2.5), being practically zero over a pH range of 3.0–2.5. Moreover, the decrease in pH, first caused a reduction in the negative zeta potential, reached zero value at pH ~4.73 (considered as OVAn pI estimation), and then became positive (Fig. 2). Results for OVAn would confirm that the decrease in net charge magnitude (derived from zeta potential values) could be responsible for the maximum OD observed around pI. Reduced net charge usually leads to a decrease in the electrostatic repulsion potential between protein macromolecules, so that attractive colloidal interactions (e.g. van de Waals and hydrophobic forces) are enhanced, promoting an increase in protein particle size by aggregation (Boye et al., 2010). This phenomenon could also explain the phase separation in OVAn system observed over a pH range of 5.5–4.0 (Fig. 3). Otherwise, it is important to note that outside of this pH range, absolute values of zeta potential were high, promoting OVAn colloidal stability by electrostatic repulsions (Boye et al., 2010).

For OVAn-PS systems, OD values were similar than the pure OVAn ones, over a pH range of 7.0–5.5, (Fig. 1), which would indicate that OD values were mainly governed by OVAn behavior. At these pH conditions, zeta potential values of OVAn-PS, OVAn and PS systems were negative (ranged from −15 to −30 mV) (Fig. 2A and B). Taking into account that over the pH range of 7.0–6.0, associative phase separation was not registered (as can be seen in Fig. 3), cosolubility phenomenon could be proposed at these conditions. This behavior can be explained by a great repulsion among biopolymer net charges (Davidov-Pardo et al., 2015). However, at pH < 6.0 mixed systems showed phase separation after 24 h (Fig. 3), suggesting that the observed turbidity could be related to the formation of big particles which sediment. Furthermore, the gradual decrease in pH promoted differences in OD and zeta potential values in OVAn-PS systems, which depended on the PS type.

For OVAn-GA systems, from pH 5.5, the decrease in pH produced an increase in OD, reaching maximum values at pH 3.5 for $R_{OVAn-GA}$ of 1:1 and at pH 3.0 for $R_{OVAn-GA}$ of 2:1 and 3.3:1 (Fig. 1). In general, this behavior could suggest the formation of OVAn-GA electrostatic complexes. Besides, Fig. 2A shows negative zeta potential values over the whole pH range due to carboxylic group dissociation of GA (branched arabinogalactan-type PS) (Weinbreck et al., 2003). Therefore, it would be appropriate to consider that attractive electrostatic interactions among OVAn positive charges and GA negative charges took place. OVAn-GA systems reached zero zeta potential at 3.73 and 2.96 for $R_{OVAn-GA}$ of 3.3:1 and 2:1, respectively. These values could be considered as pI estimations of complexes. Nevertheless, at $R_{OVAn-GA}$ of 1:1, zeta potential values remained negative and slightly higher than the pure GA ones, besides associative phase separation after 24 h was observed (Fig. 3). This finding could be explained taking into account a gradual charge neutralization, promoted by an increase in OVAn relative concentration (Fioramonti et al., 2014; Perez et al., 2015).

Similar to OVAn-GA systems, maximum OD values of OVAn-HMP systems, were found over a pH range of 3.5–3.0 (Fig. 1). However, their magnitudes were lower and practically there are no differences in OD values among the different $R_{OVAn-HMP}$. In the same way that GA, HMP showed negative zeta potential values over the whole pH range evaluated (Fig. 2). HMP is a linear polysaccharide showing negative charges conferred by carboxylic group dissociation of galacturonic acid units (de Jong & van de Velde, 2007). Hence, attractive electrostatic interactions between OVAn cationic groups and HMP anionic groups could occur. In general, zeta potential values of OVAn-HMP systems were negative following the same trend that HMP, which could suggest that net charge in mixed systems, are strongly governed by polysaccharide. An exception is the system at $R_{OVAn-HMP}$ of 3.3:1, which reached zero zeta potential at pH 2.77.

From results discussed in this section, some differences in the behavior of OVAn-GA and OVAn-HMP systems could be mentioned. Although both systems showed associative phase separation, the PS type, and the $R_{OVAn-PS}$ drove the nature of this phenomenon At pH < 5.5, OD values for OVAn-GA were higher than OVAn-HMP ones, suggesting an increased number of macromolecular entities dispersing light and/or an increase in complexes size. While, for OVAn-GA systems, at $R_{OVAn-GA}$ 3.3:1 and 2:1, was possible to estimate pI values (3.73 and 2.96, respectively) (Fig. 2A), for OVAn-HMP system only at $R_{OVAn-HMP}$ 3.3:1 a pI value could be estimated (pI 2.77) (Fig. 2B), resulting lower than the OVAn-GA ones. This behavior could be explained taking into account differences in PS charge density (number of anionic groups per PS mol). At pH > 3.5, HMP has more negative zeta potential than GA, consequently this characteristics could promote the lower OVAn-HMP zeta potential values than OVAn-GA ones (Carneiro-Da-Cunha, Cerqueira, Souza, Teixeira, & Vicente, 2011). Otherwise, OVAn would govern zeta potential in OVAn-GA systems predominantly whereas in OVAn-HMP systems, HMP would drive the electrostatic charge behavior. Finally, differences in zeta potential *versus* pH profiles could also be attributed to the differences in PS conformation (branched *versus* linear, for GA and HMP, respectively), which could have repercussions on complexes structure (Schmitt, Sanchez, Desobry-Banon, & Hardy, 1998).

3.1.2. Associative phase separation

If the aim is to obtain a dried ingredient based on PUFAs by using biopolymer nanoparticles, knowledge about the effect of variables

governing protein-polysaccharide associative phase separation could be relevant. In this sense, Fig. 3 shows that at pH < 6.0, OVAn and OVAn-PS systems present macroscopic phase separation after 24 h preparation. Therefore, this behavior could be exploited to concentrate the biopolymer of interest (Davidov-Pardo et al., 2015), in this case, OVAn.

Fig. 4A displays the effect of aqueous pH on OVAn separation yield (Y_{OVAn}, %). The highest Y_{OVAn} values were obtained over a pH range of 5.5–4.0. Then, Y_{OVAn} value decreased gradually at pH < 4.0, suggesting that the increase in OVAn positive zeta potential could promote a greater OVAn retention in solution due to electrostatic repulsion between protein net charges (Fig. 2).

On the other hand, Y_{OVAn} of OVAn-PS systems were similar to the OVAn ones, over a pH range of 7.0–4.0, registering maximum values from pH 5.5 and practically constant up to 3.0. Hence, it can be established that at this pH range (7.0–4.0), the process variables, PS type, $R_{OVAn-PS}$ and aqueous medium pH, did not produce any significant effect on Y_{OVAn} of mixed systems. However, at pH < 4.0, Y_{OVAn} values of OVAn-PS systems were higher than the OVAn without PS system, which would be explained by the associative phase separation. At pH 2.5, Y_{OVAn} values of OVAn-PS systems decreased slightly, especially for OVAn-GA systems at $R_{OVAn-GA}$ 3.3:1 and 2:1. These results are consistent with the positive zeta potential values registered for these mixed systems (Fig. 2A), which would favor OVAn retention in solution due to net charges repulsions. From a practical point of view, it is desirable to obtain the higher Y_{OVAn} values as possible. Nevertheless, in general, a Y_{OVAn} maximum of ~85% was obtained (Fig. 4A), which would indicate that ~15% OVAn remained in supernatant, and it was lost during its separation.

On the other hand, effect of aqueous medium pH on PS separation yield (Y_{PS}, %) is shown in Fig. 4B. In general, PS type, $R_{OVAn-PS}$ and aqueous medium pH affect Y_{PS} values, suggesting a great dependence on process variables. From a practical point of view, it is also desirable to obtain the highest Y_{PS} values as possible. Evidently, at pH range of 4.5–2.5, the maximum Y_{PS} values of OVAn-GA systems (53–98%) were greater than OVAn-HMP ones (34–63%), suggesting that GA addition would be more convenient than HMP. Moreover, it is important to mention that the lower $R_{OVAn-PS}$, the higher Y_{PS} values. However, this parameter does not give information about which is the PS content necessary to neutralize OVAn charges.

In order to have a better understanding, the separated PS content was also expressed related to OVAn content in the pellet (PS_p) (Fig. 4C). Consistently, PS_p values strongly depended on the process variables (PS kind, $R_{OVAn-PS}$, and aqueous medium pH). For both mixed systems, maximum PS_p values were obtained at pH 3.0, with exception of OVAn-GA system at $R_{OVAn-GA}$ 3.3:1. In general, an increase in PS_p with the decrease in $R_{OVAn-PS}$ was observed, which would be consistent with the greater relative PS amount added to mixed systems. Moreover, at the same $R_{OVAn-PS}$, OVAn-GA systems showed greater PS_p values than the OVAn-HMP ones, highlighting that more GA amount is necessary to neutralize OVAn charges, due to the lower GA charge density.

It is important to remark that the OVAn-PS systems, at $R_{OVAn-PS}$ 2:1 and 1:1, showed maximum PS_p values at maximum turbidity pH (Fig. 1). Moreover, Figs. 1 and 4C, show a similar trend with pH variation, so a relationship between PS_p and OD could be established for each system. Fig. 5 shows dispersion diagrams with linear regression model trendline. In general, a good linear correlation can be appreciated ($R^2 > 0.85$), indicating that more than 85% OD variability would be explained by PS_p variability. It is important to highlight that fitting would be specific for each system. This is more notorious for OVAn-HMP systems, which present an increase in the slope with the decrease in $R_{OVAn-HMP}$ (Fig. 5). Finally, the correlation

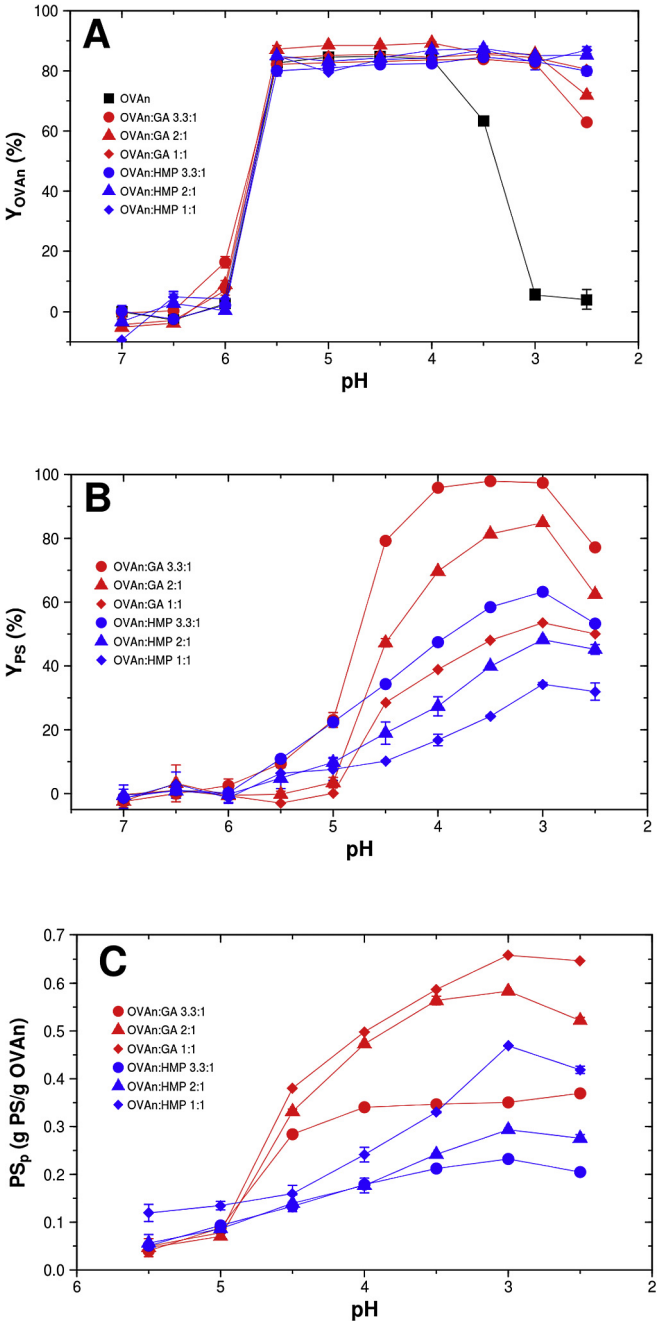

Fig. 4. **A**: Separation yield of OVAn as a function f pH for systems with and without PS. **B**: Separation yield of PS as a function of pH. **C**: PS amount in pellet relative to OVAn mass as a function of pH.

between PS_p and turbidity indicates that turbidimetric titration could be useful to estimate PS_p for a given protein-PS systems.

3.1.3. Selection of the conditions to produce LA-OVAn-PS in powder form

Based on OVAn-PS interaction results, it would be possible to select the more suitable conditions ($R_{OVAn-PS}$ and aqueous medium pH) to obtain LA-OVAn-PS powders. It is important to remark that over a pH range of 5.5–4.0, mixed systems did not show significant differences in Y_{OVAn} values (Fig. 4A). However, over a pH range of 4.0–2.5, PS addition practically maintained the maximum Y_{OVAn} value. Hence, in general, Y_{OVAn} would not be a suitable parameter to

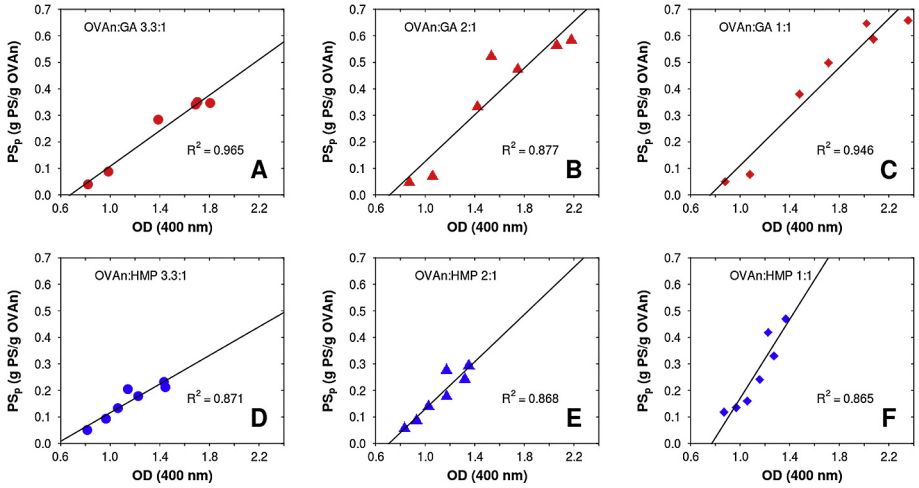

Fig. 5. Dispersion plot of PS amount in pellet *versus* turbidity (OD at 400 nm) for systems OVAn-GA and OVAn-HMP.

consider for the concentration of LA-OVAn solutions.

On the other hand, as it was previously mentioned, it is important to note that the presence of PS in the powder would be important in terms of the LA protection against deterioration factors (Perez et al., 2015; Zimet & Livney, 2009). In this sense, zeta potential measurements would help to determine a convenient $R_{OVAn\text{-}PS}$ condition to achieve protein charge neutralization, due to a complete charge neutralization could correspond to a higher electrostatic deposition of PS on OVAn. In OVAn-GA systems (Fig. 2A) relative PS amount at $R_{OVAn\text{-}PS}$ 3.3:1 and 2:1 would be not enough, because these systems showed positive zeta potential values attributable to existence of OVAn cationic groups. Hence, OVAn-GA system at $R_{OVAn\text{-}PS}$ 1:1 was chosen due to the observed net charge neutralization. Following the same criterion for OVAn-HMP systems, total neutralization of OVAn cationic groups was observed at $R_{OVAn\text{-}PS}$ 2:1 (Fig. 3B).

In relation to the selection of pH value, the criterion could be established in terms of PS_p (Fig. 4C). From a practical point of view, it can be hypothesized that maximum PS_p values would allow the maximum protection of LA-OVAn complex. In this sense, both systems, OVAn-GA at $R_{OVAn\text{-}}$1:1 $_{PS,}$ and OVAn-HMP at $R_{OVAn\text{-}PS}$ 2:1, showed the greater PS_p value at pH 3.0. For OVAn without PS, a pH value of 5.0 was chosen.

3.2. Production and characterization LA-OVAn-PS powders

As it was mentioned previously, the production process of LA-OVAn-PS in powder form consisted in: (i) formation of LA-OVAn complexes in solution, (ii) polysaccharide (PS) addition in order to concentrate LA-OVAn complexes solution via associative phase separation, and (iii) freeze-drying of separated pellet phase to obtain LA-OVAn-PS powders. A system without PS was also included. In all cases, white powders were obtained, being LA-OVAn sample less compact and more fragile than LA-OVAn-PS samples. Finally, freeze-dried powders were assayed for encapsulation parameters, water dispersibility, and LA oxidative stability, as will be discussed as follow.

3.2.1. Loading capacity, encapsulation efficiency and yield

Encapsulation parameters: loading capacity (LC), encapsulation efficiency (EE) and yield (EY) for powders of LA-OVAn with and without PS are shown in Table 1. LC parameter represents the LA_T amount contained in systems, and its knowledge would be relevant for potential formulations of functional foods. LC values of LA-OVAn-PS powders were lower than the LA-OVAn ones because PS addition would produce an increase in total solids content and so decrease in LA_T content by a "dilution" effect. Moreover, LA-OVAn-GA and LA-OVAn-HMP powders showed similar LC values ($p > 0.05$), suggesting that the PS types did not affect LA loading capacity.

On the other hand, PS addition produced a significant decrease in LA_{free} and, consequently, an increase in LA_E amount. This would mean that LA would be more inaccessible to solvent in LA-OVAn-PS powder in comparison with LA-OVAn powder. These results would have a great repercussion on EE, since higher EE values were obtained for LA-OVAn-PS powders (EE > 90%), independent of PS types. EE parameter reflects the encapsulating capacity of biopolymer materials (OVAn-PS complexes) involved in the production of LA dried ingredient. In this sense, it is important to remark that EE results would indicate that protein-polysaccharide associative phase separation enhance encapsulation properties of the biopolymer materials used in this paper (OVAn and PS).

Finally, EY parameter gives information about LA amount effectively encapsulated with respect to the amount of LA initially added and indicates LA losses over the whole nanoencapsulation process. Table 1, shows the following order for powder EY values: LA-OVAn-GA > LA-OVAn-HMP > LA-OVAn. The highest EY of LA-OVAn-GA powder corresponds to a lower LA loss (38%) over the whole nanoencapsulation process. LA losses could be attributed to an incomplete separation of LA-OVAn complexes during phase separation and so LA could be eliminated during supernatant separation. It is important to take in mind that associative phase separation process did not produce a complete OVAn separation, as it was deduced from Y_{OVAn} values in Fig. 4A, so that this fact could also lead to LA losses. Moreover, LA losses for pouring should be considered as process inherent losses, possibly due to material adhesion on recipient walls. It is important to mention that Zimet

Table 1
Loading capacity (LC); free LA (LA_{free}); encapsulated LA (LA_E); encapsulation efficiency (EE) and encapsulation yield (EY). Values presented as mean ± standard deviation (n = 3).

Sistema	LC (%)	LA_{free} (%)	LA_E (%)	EE (%)	YE (%)
LA-OVAn	19.10 ± 1.34 (b)	12.20 ± 2.04 (b)	6.90	36.11	27.09
LA-OVAn-GA	10.63 ± 0.54 (a)	0.73 ± 0.20 (a)	9.90	93.09	62.81
LA-OVAn-HMP	10.83 ± 0.01 (a)	0.70 ± 0.15 (a)	10.13	93.58	56.29

Different letters indicate a statistically significant difference ($p < 0.05$).

and Livney (2009) obtained 64% EY for DHA encapsulation, using β-lactoglobulin and low methoxyl pectin as encapsulation biopolymer materials. Although they did not produce nano-encapsulated DHA powders, DHA losses were attributed to centrifugation and pellet separation steps.

3.2.2. Water dispersibility assay

After 24 h hydration, systems showed the following pH values for LA-OVAn, LA-OVAn-GA and LA-OVAn-HMP: 5.40, 3.76 and 3.69, respectively. These pH values were slightly greater than pH used for associative phase separation (5.0 for LA-OVAn and 3.0 for LA-OVAn-PS systems). In addition, the presence of big aggregates was observed (in agreement with results discussed in section 3.1.1), even after pH adjustment to 7.0 (Fig. 6). The limited dispersibility of powders at neutral pH could be explained considering protein aggregate formation over freeze-drying step. Usually, insoluble protein aggregates formation over freeze-drying process is attributable to intermolecular disulfide bonds formation, and other cross-linking reactions, e.g. dityrosine formation. Moreover, drying step removes hydration water, which could promote protein conformational changes (Wang, 2005). Another cause of aggregation could be attributable to a rapid hydration of powder in aqueous medium, which could not allow to the dried protein to rehydrate as slowly as the dehydration step, producing aggregation (Wang, 2000).

It is noteworthy that LA-OVAn-HMP powder presented the lowest amount of insoluble aggregated material (Fig. 6), producing a slight turbid dispersion. In order to remove insoluble material, LA-OVAn-HMP dispersion was centrifuged. Then, PSD analysis was performed on supernatant. PSD based on intensity, volume and number (PSDi, PSDv and PSDn, respectively) are shown in Fig. 7A, B and C, respectively. Fig. 7A, shows a bimodal PSD with a considerable overlap between two populations of particle size. Each peak has a value of 77 nm and 406 nm. The first one would correspond to LA-OVAn, in agreement with results reported in Sponton et al. (2015a), whereas the other peak would correspond to biopolymer aggregates. The presence of non-aggregated OVAn would suggest a considerable colloidal stability of re-hydrated powder particles. This behavior could be attributed, in first place to repulsive interaction between OVAn and HMP, because both biopolymer are negatively charged at neutral pH (Fig. 2B), contributing to LA-OVAn dispersion due to a cosolubility behavior (Davidov-Pardo et al., 2015). In second place, to a protective effect of HMP against protein aggregation induced during freeze-drying process. This finding evidences a better cryoprotectant effect of HMP than GA during freeze-drying process.

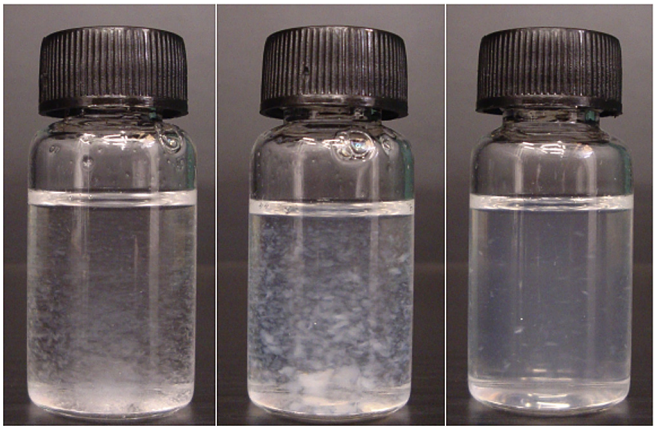

Fig. 6. Visual appearance of suspended powders (2 g/L) in deionized water at pH 7.0. LA-OVAn (left), LA-OVAn-GA (center) and LA-OVAn-HMP (right).

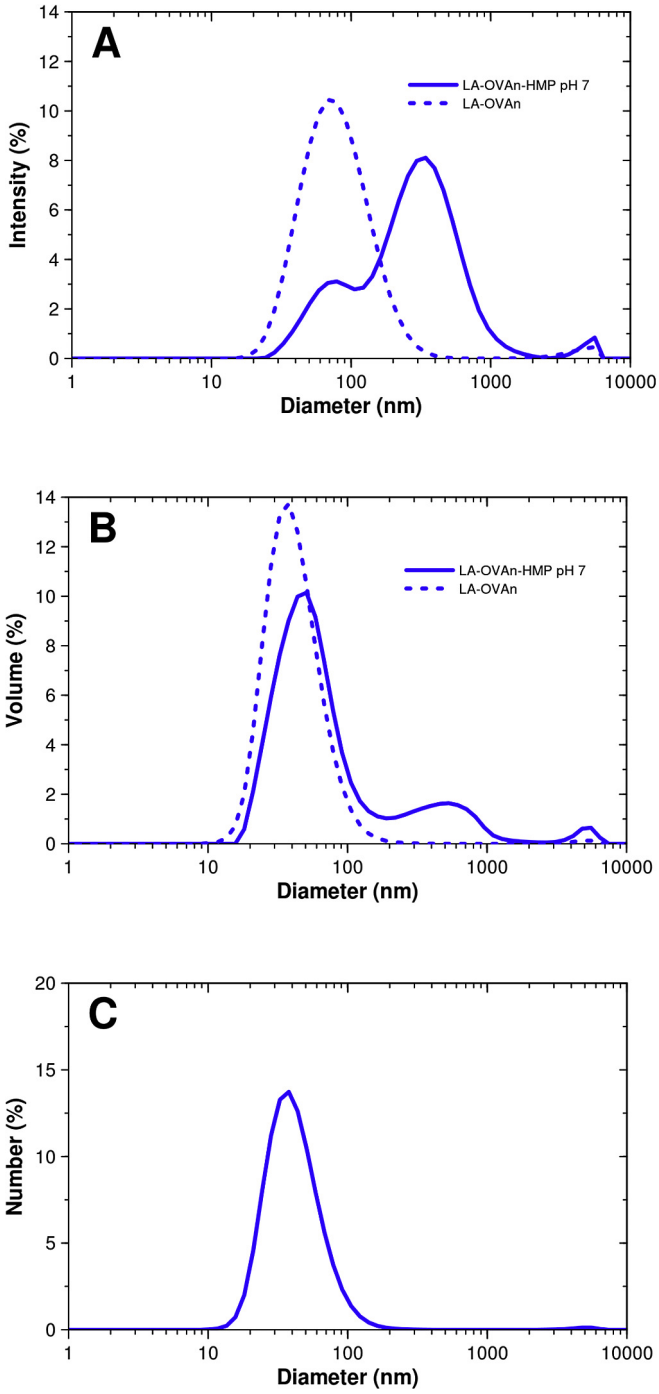

Fig. 7. Particle size distribution (**A**: intensity, **B**: volume, **C**: number) of LA-OVAn-HMP after dispersion and centrifugation.

3.2.3. Oxidative stability of linoleic acid

Evolution of the oxidative stability for LA in freeze-dried powders is shown in Fig. 8. LA remains non-deteriorated (LA_{ND}) for 2 days, in the samples of LA-OVAn and LA-OVAn-HMP powders. However, LA-OVAn-GA powder showed a strong decrease in LA_{ND}, producing ~30% loss over the same examined period. After 2 days, LA_{ND} showed the following order: LA-OVAn-HMP > LA-OVAn > LA-OVAn-GA. At 13 day, LA-OVAn-HMP powder showed ~20% LA deterioration, whereas LA-OVAn and LA-OVAn-GA powders showed 70% and 95% LA deterioration, respectively. These results

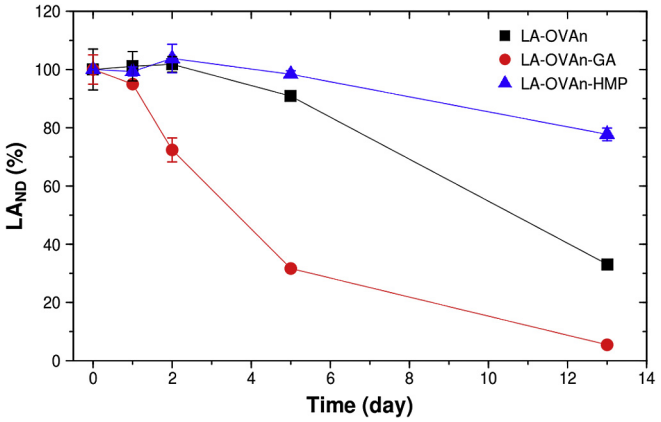

Fig. 8. Non deteriorated LA in systems LA-OVAn with and without PS as a function of storage time at 40 °C.

demonstrated that HMP promotes a considerable oxidative stability of LA in freeze-dried powders, in contrast to GA.

It is important to highlight that, taking into account the high EE values of LA-OVAn-PS, compared to LA-OVAn (Table 1), a greater protective effect would be expected in powders based on PS. However, this behavior was only registered for LA-OVAn-HMP system. Hence, although GA promoted greater solvent inaccessibility, it would promote higher oxygen accessibility during storage period, leading to oxidative deterioration.

According to technological performance observed in the analyzed systems, LA-OVAn-HMP powder would be the appropriate one to be used as ingredient for LA incorporation in foods. Because of their water dispersibility behavior, applications in aqueous systems requiring colloidal stability (e.g., clear beverages) could be limited. However, it could find applications in beverages that allowing some level of particle sedimentation, e.g. fruit pulp juices, which often require shaking before consumption. Moreover, powder ingredient would find applications in no liquid food matrices, such as dairy and bread products, etc. Performance of LA powder ingredient in food matrices would be informed in a forthcoming paper.

4. Conclusion

This paper presents experimental information about OVAn-PS associative phase separation in order to produce nano-encapsulated linoleic acid (LA) in powder form. Process variables: PS types (GA or HMP), $R_{OVAn:PS}$ and aqueous medium pH, exert key roles on separation yield of OVAn (Y_{OVAn}) and PS (Y_{PS}), and besides on PS content needed to concentrate OVAn (PS_p). The more adequate conditions to obtain LA-OVAn-PS powders were: $R_{OVAn:PS}$ 1:1 and 2:1 (OVAn-GA and OVAn-HMP systems, respectively) and pH 3.0. Freeze-dried powders showed differences in water dispersion behavior and LA oxidative stability, mainly depending on PS types. LA-OVAn-HMP powder showed better water dispersion behavior and the highest LA oxidative stability, becoming in a promising system to produce a dried ingredient based on LA.

In conclusion, associative phase separation would be a convenient strategy to concentrate biopolymer nanoparticles in solution and, subsequently, to produce encapsulated PUFAs powders. This technology would offer potential applications for nano-encapsulation of other lipophilic bioactive compounds.

Acknowledgements

Authors acknowledge the financial support of the following projects: CAI+D-2013-50120110100-171-LI (UNL) and PICT-2014-2636 (ANPCyT), and especially to CONICET – Argentina for the PhD fellowships awarded to Osvaldo E. Sponton. Authors also acknowledge to Patricia Zimet for their technical advices on chromatographic experiments.

References

Agbenorhevi, J. K., & Kontogiorgos, V. (2010). Polysaccharide determination in protein/polysaccharide mixtures for phase-diagram construction. *Carbohydrate Polymers, 81*(4), 849–854.
Boye, J. I., Aksay, S., Roufik, S., Ribéreau, S., Mondor, M., Farnworth, E., et al. (2010). Comparison of the functional properties of pea, chickpea and lentil protein concentrates processed using ultrafiltration and isoelectric precipitation techniques. *Food Research International, 43*(2), 537–546.
Carneiro-Da-Cunha, M. G., Cerqueira, M. A., Souza, B. W. S., Teixeira, J. A., & Vicente, A. A. (2011). Influence of concentration, ionic strength and pH on Zeta potential and mean hydrodynamic diameter of edible polysaccharide solutions envisaged for multinanolayered films production. *Carbohydrate Polymers, 85*(3), 522–528.
Davidov-Pardo, G., Joye, I. J., & McClements, D. J. (2015). Food-grade protein-based nanoparticles and microparticles for bioactive Delivery: Fabrication, characterization, and utilization. *Advances in Protein Chemistry and Structural Biology, 98*, 293–325.
David, S., Zagury, Y., & Livney, Y. D. (2015). Soy β-conglycinin–curcumin nanocomplexes for enrichment of clear beverages. *Food Biophysics, 10*(2), 195–206.
Dubois, M., Gilles, K. A., Hamilton, J. K., Rebers, P. A. Y., & Smith, F. (1956). Colorimetric method for determination of sugars and related substances. *Analytical Chemistry, 28*(3), 350–356.
Fioramonti, S. A., Perez, A. A., Aringoli, E., Rubiolo, A. C., & Santiago, L. G. (2014). Design and characterization of soluble biopolymer complexes produced by electrostatic self-assembly of a whey protein isolate and sodium alginate. *Food Hydrocolloids, 35*, 129–136.
Gallardo, G., Guida, L., Martinez, V., López, M. C., Bernhardt, D., Blasco, R., et al. (2013). Microencapsulation of linseed oil by spray drying for functional food application. *Food Research International, 52*(2), 473–482.
Hartree, E. F. (1972). Determination of protein: A modification of the Lowry method that gives a linear photometric response. *Analytical Biochemistry, 48*, 422–427.
Humblet-Hua, K. N. P., Scheltens, G., van der Linden, E., & Sagis, L. M. C. (2011). Encapsulation systems based on ovalbumin fibrils and high methoxyl pectin. *Food Hydrocolloids, 25*(4), 569–576.
de Jong, S., & van de Velde, F. (2007). Charge density of polysaccharide controls microstructure and large deformation properties of mixed gels. *Food Hydrocolloids, 21*(7), 1172–1187.
Joye, I. J., Davidov-Pardo, G., Ludescher, R. D., & McClements, D. J. (2015). Fluorescence quenching study of resveratrol binding to zein and gliadin: Towards a more rational approach to resveratrol encapsulation using water-insoluble proteins. *Food Chemistry, 185*, 261–267.
Joye, I. J., & McClements, D. J. (2014). Biopolymer-based nanoparticles and microparticles: Fabrication, characterization, and application. *Current Opinion in Colloid & Interface Science, 19*, 417–427.
Kehoe, J. J., & Brodkorb, A. (2014). Interactions between sodium oleate and α-lactalbumin: The effect of temperature and concentration on complex formation. *Food Hydrocolloids, 34*, 217–226.
de Kruif, C. G., Weinbreck, F., & De Vries, R. (2004). Complex coacervation of proteins and anionic polysaccharides. *Current Opinion in Colloid and Interface Science, 9*(5), 340–349.
Li, Z., Gu, T., Kelder, B., & Kopchick, J. J. (2001). Analysis of fatty acids in mouse cells using reversed-phase high-performance liquid chromatography. *Chromatographia, 54*(7/8), 463–467.
Li, X., Liu, Y., Li, N., Xie, D., Yu, J., Wang, F., et al. (2016). Studies of phase separation in soluble rice protein/different polysaccharides mixed systems. *LWT - Food Science and Technology, 65*, 676–682.
McClements, D. J. (2006). Non-covalent interactions between proteins and polysaccharides. *Biotechnology Advances, 24*, 621–625.
Niu, F., Su, Y., Liu, Y., Wang, G., Zhang, Y., & Yang, Y. (2014). Ovalbumin-gum Arabic interactions: Effect of pH, temperature, salt, biopolymers ratio and total concentration. *Colloids and Surfaces B: Biointerfaces, 113*, 477–482.
Perez, A. A., Andermatten, R. B., Rubiolo, A. C., & Santiago, L. G. (2014). β-Lactoglobulin heat-induced aggregates as carriers of polyunsaturated fatty acids. *Food Chemistry, 158*, 66–72.
Perez, A. A., Sponton, O. E., Andermatten, R. B., Rubiolo, A. C., & Santiago, L. G. (2015). Biopolymer nanoparticles designed for polyunsaturated fatty acid vehiculization: Protein–polysaccharide ratio study. *Food Chemistry, 188*, 543–550.
Ptaszek, P., Kabziński, M., Kruk, J., Kaczmarczyk, K., Źmudziński, D., Liszka-Skoczylas, M., et al. (2015). The effect of pectins and xanthan gum on physicochemical properties of egg white protein foams. *Journal of Food Engineering, 144*, 129–137.
Santiago, L. G., & Castro, G. R. (2016). Novel technologies for the encapsulation of bioactive food compounds. *Current Opinion in Food Science, 7*, 78–85.
Schmitt, C., Sanchez, C., Desobry-Banon, S., & Hardy, J. (1998). Structure and techno

functional properties of protein-polysaccharide complexes: A review. *Critical Reviews in Food Science and Nutrition, 38*, 689–753.

Semenova, M. (2016). Advances in molecular design of biopolymer-based delivery micro/nanovehicles for essential fatty acids. *Food Hydrocolloids*. http://dx.doi.org/10.1016/j.foodhyd.2016.09.019.

Spada, J. C., Marczak, L. D. F., Tessaro, I. C., & Cardozo, N. S. M. (2015). Interactions between soy protein from water-soluble soy extract and polysaccharides in solutions with polydextrose. *Carbohydrate Polymers, 134*(10177), 119–127.

Sponton, O. E., Perez, A. A., Carrara, C. R., & Santiago, L. G. (2015a). Linoleic acid binding properties of ovalbumin nanoparticles. *Colloids and Surfaces B: Biointerfaces, 128*, 219–226.

Sponton, O. E., Perez, A. A., Carrara, C. R., & Santiago, L. G. (2015b). Impact of environment conditions on physicochemical characteristics of ovalbumin heat induced nanoparticles and on their ability to bind PUFAs. *Food Hydrocolloids, 48*, 165–173.

Sponton, O. E., Perez, A. A., Carrara, C. R., & Santiago, L. G. (2016). Complexes between ovalbumin nanoparticles and linoleic acid: Stoichiometric, kinetic and thermodynamic aspects. *Food Chemistry, 211*, 819–826.

Wang, W. (2000). Lyophilization and development of solid protein pharmaceuticals. *International Journal of Pharmaceutics, 203*, 1–60.

Wang, W. (2005). Protein aggregation and its inhibition in biopharmaceutics. *International Journal of Pharmaceutics, 289*(1–2), 1–30.

Weinbreck, F., de Vries, R., Schrooyen, P., & de Kruif, C. G. (2003). Complex coacervation of whey proteins and gum Arabic. *Biomacromolecules, 4*(2), 293–303.

Wicker, L., Kim, Y., Kim, M.-J., Thirkield, B., & Lin, Z. (2014). Pectin as a bioactive polysaccharide e Extracting tailored function from less. *Food Hydrocolloids, 42*, 251–259.

Zimet, P., & Livney, Y. D. (2009). Beta-lactoglobulin and its nanocomplexes with pectin as vehicles for omega-3 polyunsaturated fatty acids. *Food Hydrocolloids, 23*, 1120–1126.